

PVT-x Behavior of He-N₂ Mixtures from 270 to 353 K and up to 280 bar

Wei Zhang* and Jan A. Schouten

Van der Waals-Zeeman Laboratorium, Universiteit van Amsterdam, Valkenierstraat 67, 1018 XE Amsterdam, The Netherlands

Helno M. Hinze and Manfred Jaeschke

Ruhrgas AG, Halterner Strasse 125, D-4270 Dorsten 21, Federal Republic of Germany

The compressibility factor of He-N₂ mixtures was measured with a Burnett setup and an optical apparatus in the pressure range up to 280 bar and the temperature range from 270 to 353 K. The pure and unlike second and third virial coefficients and their dependence on temperature were derived from the experimental data.

1. Introduction

The number of investigations concerning the thermodynamic behavior of binary mixtures at high pressure is very limited. Moreover, the applications of high-pressure technology is increasing rapidly, and the data of thermodynamic properties of mixtures at high pressure are important to these applications. It is well-known that the unlike interactions cannot be accurately determined from the interactions in pure substances. Therefore, the information on the equation of state of binary mixtures is indispensable in determining the thermodynamic properties of a binary system and the effective pair potentials, in particular, the repulsive part.

This investigation is part of a systematic study of the PVT-x properties of binary mixtures of helium and nitrogen up to 10 kbar at the Van der Waals-Zeeman Laboratory. The interest in this particular binary system is due not only to the simple shapes of both helium and nitrogen molecules but also to the relatively large difference in size and mass of these molecules. These would allow an easier approach to acquire knowledge of unlike interactions and to compare existing theories for fluid mixtures with experimental data. Moreover, the internal degree of freedom in the nitrogen molecule gives a more complicated phase diagram and plays a role in a very interesting behavior of the helium-nitrogen mixture in the solid phase (1), although the nitrogen molecule is almost spherical. To explain these phenomena, the knowledge of the unlike interactions is essential.

The experiments on the compressibility factor of this binary system as well as pure helium were carried out in Ruhrgas AG, Dorsten, West Germany, with a Burnett setup and an optical apparatus consisting of interferometers (2). More details about the experiments and the experimental compressibility factor of pure nitrogen have been published elsewhere (3, 4).

2. Experimental Methods

Burnett and optical experiments were used to measure the compressibility factor of pure helium and mixtures of 24.940, 49.964, and 74.911 mol % helium. The data were collected along isotherms in the temperature range from 270 to 353 K and the pressure range up to 280 bar. The optical experiment allows quick measurement, but it needs the Burnett experiment for a precise calibration; therefore, both methods were used in this work.

2.1. Burnett Experiment. Since the setups have been described elsewhere (2), we will give here only an outline of the method.

The Burnett setup consists of vessels A and B (Figure 1). Vessel A is connected to a gas compressor through valve 1 and also connected to a dead-weight pressure balance by a differential pressure meter (DPM). Vessel B is connected to a vacuum pump through valve 2. Moreover vessels A and B are connected through expansion valve 3. All these parts are in a thermostat bath in which the temperature can be stabilized within 0.01 K and can be measured with a mercury thermometer.

One can start the experiment by filling vessel A up to 280 bar, while keeping vessel B at high vacuum, and then close valve 1. After the gas in vessel A reaches thermal equilibrium with the thermostat bath, the pressure in vessel A is measured with the dead-weight balance. The procedure is then as follows: the gas in vessel A is released into vessel B. When the gas in vessels A and B reaches mechanical and thermal equilibrium, the pressure is measured with the dead-weight pressure balance and the expansion valve 3 is then closed. The vessel B is evacuated to high vacuum, and the above procedure is repeated. The experiment is finished when the gas pressure reaches the lower limit of the accurate pressure measurement (about 1 bar).

By analyzing the experimental procedure and applying the mass conservation principle, one can derive the following formula to calculate the compressibility factor after the *j*th expansion of the sample gas:

$$Z_j = P_j \frac{Z_0}{P_0} \prod_{i=1}^j \frac{(V_A + V_B)_i}{(V_A)_{i-1}} \quad (1)$$

It is obvious that the volumes V_A and V_B would expand under pressure, and therefore we apply a linear Taylor expansion to the distorted volumes $(V_A + V_B)_i$ and $(V_A)_{i-1}$. Equation 1 then becomes

$$Z_j = P_j \frac{Z_0}{P_0} \prod_{i=1}^j \frac{(V_A + V_B)^0 (1 + aP_i)}{(V_A)^0 (1 + bP_{i-1})} \quad (2)$$

where $N^0 = (V_A + V_B)^0 / (V_A)^0$ is the zero-pressure cell constant. The parameters *a* and *b* are those of a Taylor expansion around zero pressure and are independent of temperature. The cell constant N^0 and the run constant Z_0/P_0 can be calculated by applying the

$$\frac{(V_A + V_B)^0}{(V_A)^0} = \lim_{P_j \rightarrow 0} \frac{P_{j-1}}{P_j} \quad (3)$$

$$\frac{P_0}{Z_0} = \lim_{P_j \rightarrow 0} P_j \prod_{i=1}^j \frac{(V_A + V_B)^0 (1 + aP_i)}{(V_A)^0 (1 + bP_{i-1})} \quad (4)$$

2.2. Optical Experiment. The optical setup consists of one measuring interferometer and one pressure interferometer, which are installed in different thermostats. Each interferometer consists of a measuring cell and a reference cell. Both measuring cells are connected to a pressure equilibrium

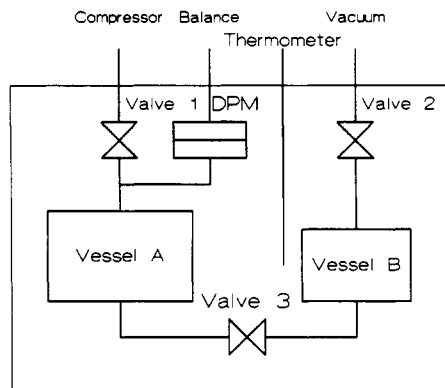


Figure 1. Burnett setup: differential pressure meter (DPM); dead-weight balance; gas compressor; mercury thermometer; vacuum system; valve 1; valve 2; valve 3; vessel A; vessel B.

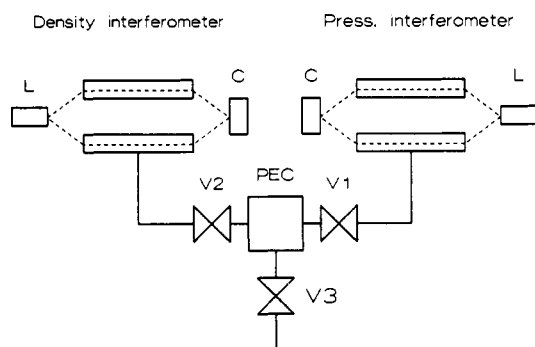


Figure 2. Optical setup: C, L, and V represents signal converter (C); laser (L); valve (V); pressure equilibrium chamber (PEC).

chamber (PEC) through valve 1 and valve 2, as shown in Figure 2.

Both interferometers work as follows (see Figure 2). A laser beam is split by a diffraction grating into a measuring beam and a coherent reference one. After traveling through the measuring cell filled with gas and the reference cell kept at high vacuum, these two coherent beams are focused on a signal converter C and display interference which is recorded by a fringe counter. If the optical path length differs by 1 wavelength, a full bright-dark-bright change in the interference fringes occurs. The refractive index is measured by counting the changes in the interference fringes caused by the density changes of the gas.

$$n - 1 = \lambda k L^{-1} \quad (5)$$

where n is the refractive index, λ is the wavelength of the laser, k is the fringe number, and L is the cell length.

The density of the sample gas can be determined from the measured refractive index by the Lorentz-Lorenz law

$$\frac{n^2 - 1}{n^2 + 2} \frac{1}{\rho} = A_n + B_n \rho + C_n \rho^2 + \dots \quad (6)$$

where A_n , B_n , C_n , ... are refractive virial coefficients. A_n has been directly determined from the measured refractive index by plotting $(n^2 - 1)/[(n^2 + 2)P]$ as a function of pressure at ideal gas condition $P = 0$. The B_n and C_n have been determined by a least-squares fit against the Burnett measurement. It should be noted that A_n weighs over 99% in the total contribution of all the terms in the right-hand side of eq 6, and therefore the dependence of the optical experiment upon the Burnett one is very weak.

Since the pressure interferometer has been calibrated with pure nitrogen against a dead-weight balance and the density of nitrogen is accurately known, one can determine the pressure in the measuring cell from the refractive index of pure nitrogen.

Table I. Experimental Refractive Virial Coefficients

helium/ (mol %)	A_n / (cm^3/mol)	ΔA_n / (cm^3/mol)	B_n / (cm^6/mol^2)	C_n / (cm^9/mol^3)
100.000	0.5206	0.0006	-0.16	6
74.911	1.5048	0.0008	-0.05	-7
49.964	2.4852	0.0016	0.11	-32
24.940	3.4674	0.0016	0.33	-61
0.000	4.4465	0.0018	0.60	-85

One can start the optical experiment by filling the measuring cell of the measuring interferometer with sample gas and that of the pressure interferometer with pure nitrogen up to 280 bar and then manipulate valves 1, 2, and 3 in such a way that both gases expand into the PEC and reach both mechanical and thermal equilibrium. So the pressures in both cells are the same and can be calculated from the refractive index of pure nitrogen. One should measure the temperature and the refractive indexes of both sample gas and pure nitrogen. Then one can open valve 3 to release some gases to reach lower pressure and close valve 3 and measure the same quantities after both gases reach equilibrium again. This procedure is repeated until the pressure in the cells of both interferometers is very low.

2.3. The Uncertainty of Measurements. The temperature was controlled and measured with platinum resistance and mercury thermometers in both Burnett and optical experiments. The uncertainty of the temperature measurements is 0.01 K.

The dead-weight pressure balance in the Burnett setup measures pressure with an uncertainty of 0.0006 bar in the range from 1 to 6 bar and 0.01% above 6 bar. The pressure interferometer of the optical experiment measures pressure with an uncertainty of 0.0009 bar in the range from 1 to 6 bar and 0.015% above 6 bar.

The uncertainties of the cell constant and run constant of the Burnett experiment are 0.001 and 0.05%, respectively. The uncertainties of the refractive index and the A_n value of the optical experiment are 0.0015 and 0.05%. The refractive virial coefficients used in this work to calculate the compressibility factor from eq 6 are listed in Table I.

The concentrations of helium in this binary system are 100.000, 74.911, 49.964, 24.940, and 0.000 mol%. The sample gas for this work was purchased from Messer Griesheim, and the maximum uncertainty of the concentration of helium in the binary mixtures is claimed to be less than 0.008 mol%.

Taking into account these uncertainties, one can derive that the overall uncertainty of the compressibility factor of the Burnett experiment is 0.07% from 6 to 80 bar and 0.10% above 80 bar. The optical experiment is consistent with the Burnett experiment within 0.03%, as indicated in Table II in the lines denoted by superscript B.

3. Results

3.1. Experimental Results. The compressibility factor along each isotherm determined by the Burnett and optical methods can be presented by a polynomial expression in density as follows

$$Z = 1 + c_1 \rho + c_2 \rho^2 + c_3 \rho^3 \quad (7)$$

and the coefficients c_i ($i = 1, 2, \text{ and } 3$) of each isotherm and the percentage standard deviation of each fit are given in Table II. For each isotherm the number of data points is about 55, except for those along which both Burnett and optical measurements have been performed in which cases the numbers ranged from 65 to 90. Since the standard deviation for those isotherms, where the Burnett and optical results are fitted simultaneously, is equal to or less than 0.03%, it is obvious that the Burnett measurements are consistent with the optical

Table II. Coefficients for Equation 7

helium/ (mol %)	T/ K	C ₁ / (cm ³ /mol)	C ₂ / (cm ⁶ /mol ²)	C ₃ / (cm ⁹ /mol ³)	100σ ^{a,b} / %
100.000	273.15	11.896	109.6	108	0.005 ^B
100.000	393.15	11.819	99.5	184	0.006 ^B
100.000	313.15	11.747	96.9	157	0.006 ^B
100.000	330.00	11.728	72.8	344	0.005 ^B
100.000	353.15	11.632	67.8	371	0.006 ^B
74.911	270.00	13.949	270.0	548	0.006
74.911	290.00	14.267	274.0	482	0.005
74.911	298.15	14.613	233.7	688	0.005 ^B
74.911	310.00	14.727	227.4	745	0.007
74.911	330.00	14.841	268.0	425	0.004
74.911	350.00	15.174	236.1	601	0.002
49.964	270.00	10.929	491.5	1395	0.005
49.964	290.00	11.824	553.8	954	0.004 ^B
49.964	310.00	12.752	579.0	747	0.009 ^B
49.964	330.00	13.852	563.4	761	0.007
24.940	270.00	2.636	816.1	2768	0.006
24.940	290.00	5.273	800.1	2713	0.006
24.940	298.15	6.010	840.1	2404	0.007 ^B
24.940	310.00	7.564	778.7	2697	0.004
24.940	330.00	9.450	767.5	2691	0.003
24.940	350.00	11.085	767.0	2608	0.003
0.000	269.30	-10.589	1165.4	5179	0.023
0.000	273.15	-9.727	1162.1	5223	0.030 ^B
0.000	290.00	-6.069	1160.1	4986	0.016
0.000	293.15	-5.507	1173.0	4898	0.016 ^B
0.000	310.00	-2.345	1150.0	4891	0.010
0.000	313.15	-1.807	1145.8	4911	0.013 ^B
0.000	323.15	-0.170	1140.1	4869	0.010
0.000	330.00	0.874	1142.3	4789	0.008
0.000	350.00	3.681	1136.0	4670	0.006 ^B
0.000	353.15	4.092	1132.7	4690	0.007 ^B

^a Standard deviation of each fit. ^b Superscript B denotes the fit with data points of both Burnett and optical measurements.

measurements within the experimental uncertainty.

However, the raw data of compressibility factor of pure helium as well as the binary mixtures of helium and nitrogen are presented in the supplementary material. The nitrogen data have been published elsewhere (3, 4).

3.2. Pure and Interaction Virial Coefficients. The experimental compressibility factors have been analyzed by applying the virial equation of state along each isotherm.

$$Z = 1 + B\rho + C\rho^2 + D\rho^3 + E\rho^4 \quad (8)$$

The second virial coefficient B and third virial coefficient C were determined at each temperature by a least-squares fit of the virial equation against the experimental compressibility factor. The fit was carried out by including successively more data points and more coefficients according to the scheme proposed by Van den Berg (5).

Since the virial coefficients are only dependent on the temperature of the gas, the standard deviation of the fit should not systematically increase. As soon as that happens, a higher power of the density is included in the expression. On each isotherm, the least-squares fit was carried out on the virial equation, including initially two terms against the experimental data, starting from the first six data points of lowest pressure. This was then repeated with the same number of terms each time after one more data point of higher pressure was added. The fit was considered consistent until a systematic increase of the standard deviation occurred or until the virial coefficients determined by the fit went beyond the uncertainties of virial coefficients determined in the preceding fit at the same temperature. Then one higher order term was added to the virial equation, and above-mentioned procedure was started again. The fitting process of one isotherm was continued until five terms of the virial equation were used.

The application of these criteria in determining the second and third virial coefficients is demonstrated in Figures 3 and 4,

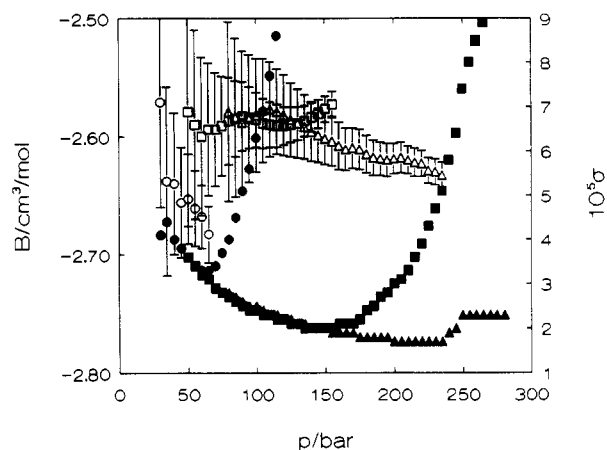


Figure 3. Second virial coefficients of pure nitrogen at 310.00 K. Open symbols stand for values of second virial coefficients, and filled ones represent the standard deviation of each fit. Error bars associated with the open symbols, representing only random errors of the experiment, were mathematically determined from the fitting procedures. Circles, squares, and triangles denote three-term, four-term, and five-term fits of the virial equation of state, respectively.

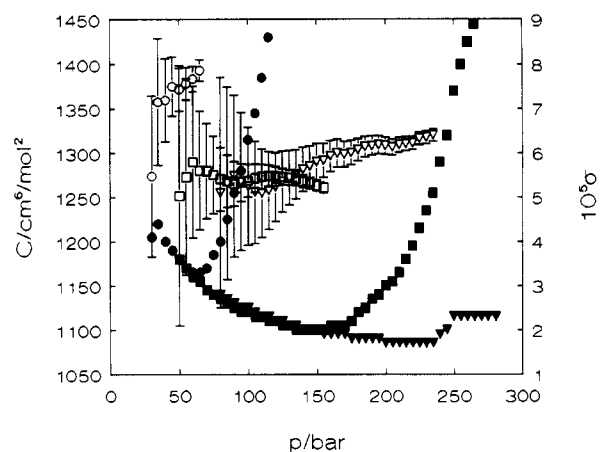


Figure 4. Third virial coefficients of pure nitrogen at 310.00 K. Open symbols stand for values of third virial coefficients, and filled ones represent the standard deviation of each fit. Error bars associated with the open symbols, representing only random errors of the experiment, were mathematically determined from the fitting procedures. Circles, squares, and triangles denote three-term, four-term, and five-term fits of the virial equation of state, respectively.

where the values for B and C are plotted along the left vertical axis, the values for the standard deviation of the fit along the right vertical axis, and the pressure along the horizontal axis. Filled circles, squares, and triangles represent the standard deviation of the fit of the virial equation of three, four, and five terms respectively, and open symbols stand for the values of B and C following the same sequence. A systematic increase of the standard deviation of the fit indicates the demand for a higher order term in the virial equation in order to obtain significant values of B and C . These two figures also demonstrate that the values of B and C determined with virial equations of three, four, and five terms are consistent within their uncertainties.

The values of second and third virial coefficients given in Table III are the averages of all the significant virial coefficients at the same temperature determined with a three-term virial equation of state, e.g., the averages of values denoted by the open circles in Figures 3 and 4 give respectively the second and third virial coefficients listed in Table III. This treatment made the virial coefficients of pure nitrogen presented in Table III somewhat different from those published elsewhere (3, 4, 7), which are the significant virial coefficients at highest pressure before the systematic increase of standard deviation in the

Table III. Experimental Second and Third Virial Coefficients

helium/ (mol %)	T/ K	B ^a / (cm ³ /mol)	C ^a / (cm ⁶ /mol ²)
100.000	273.15	11.90	111
100.000	293.15	11.78	120
100.000	313.15	11.73	109
100.000	330.00	11.75	74
100.000	353.15	11.61	87
74.911	270.00	13.91	297
74.911	290.00	14.23	301
74.911	298.15	14.61	260
74.911	310.00	14.69	263
74.911	330.00	14.83	284
74.911	350.00	15.14	260
49.964	270.00	10.95	513
49.964	290.00	11.70	627
49.964	310.00	12.65	639
49.964	330.00	13.75	624
24.940	270.00	2.57	888
24.940	290.00	5.21	860
24.940	298.15	5.81	983
24.940	310.00	7.56	842
24.940	330.00	9.47	785
24.940	350.00	11.10	791
0.000	269.30	-11.18	1480
0.000	273.15	-10.23	1440
0.000	290.00	-6.46	1400
0.000	293.15	-5.87	1420
0.000	310.00	-2.65	1360
0.000	313.15	-2.07	1350
0.000	323.15	-0.40	1300
0.000	330.00	0.64	1320
0.000	350.00	3.64	1220
0.000	353.15	3.92	1290

^aThe uncertainties of *B* and *C* are estimated to be 0.20 cm³/mol and 100 cm⁶/mol², respectively.

Table IV. Interaction Second Virial Coefficients B₁₂

helium/ (mol %)	T/ K	B ₁₂ / (cm ³ /mol)	helium/ (mol %)	T/ K	B ₁₂ / (cm ³ /mol)
74.911	270.00	21.1	49.964	310.00	20.7
74.911	290.00	21.3	49.964	330.00	21.3
74.911	298.15	22.1	24.940	270.00	21.4
74.911	310.00	22.0	24.940	290.00	21.8
74.911	330.00	21.9	24.940	298.15	20.9
74.911	350.00	22.3	24.940	310.00	22.2
49.964	270.00	21.5	24.940	330.00	22.3
49.964	290.00	20.8	24.940	350.00	22.4

fitting occurs. But the discrepancy is within the experimental accuracy.

Since the second virial coefficients of the three mixtures and two pure components are now available (see Table III), the interaction second virial coefficient *B*₁₂ could be determined with the mixing rule

$$B_{\text{mix.}} = x_1^2 B_1 + 2x_1 x_2 B_{12} + x_2^2 B_2 \quad (9)$$

where subscripts 1 and 2 denote helium and nitrogen, respectively. The values of interaction second virial coefficient are given in Table IV.

But the values of the interaction third virial coefficients could not be directly determined with the mixing rule

$$C_{\text{mix.}} = x_1^3 C_1 + 3x_1^2 x_2 C_{112} + 3x_1 x_2^2 C_{122} + x_2^3 C_2 \quad (10)$$

The values of *C*₁₁₂ and *C*₁₂₂ have been determined using all the *C* values of mixture in Table III from eq 10. It turns out that *C*₁₁₂ and *C*₁₂₂ are constant within the experimental accuracy. The second virial coefficients in Tables III and IV are also represented by the functions of temperature. Since the results at 350.00 K for the mixture of 49.964 mol % helium are

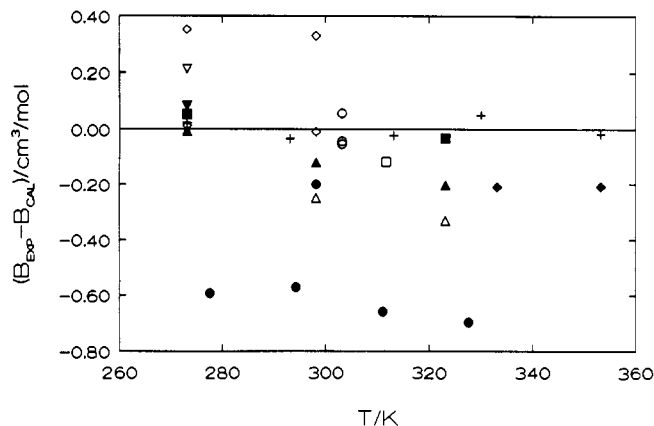


Figure 5. Comparison of the second virial coefficients of pure helium from this work, as well as those from literature, with those calculated using the temperature dependence, eq 11: Δ , ref 8; \blacktriangle , ref 9; \circ , ref 10; \bullet , ref 11; ∇ , ref 12; \blacktriangledown , ref 13; \square , ref 14; \blacksquare , ref 15; \diamond , ref 16; \blacklozenge , ref 17; $+$, this work.

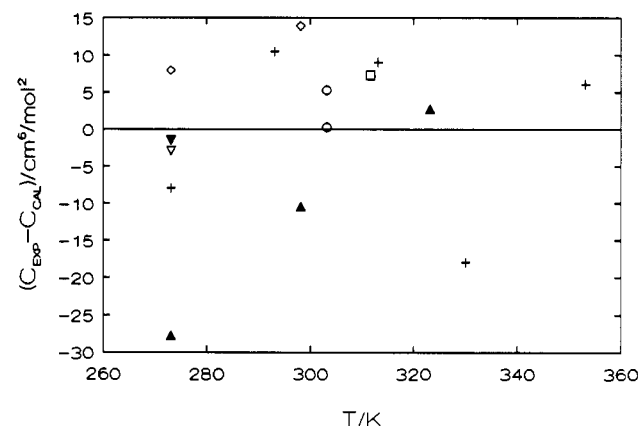


Figure 6. Comparison of the third virial coefficients of pure helium from this work, as well as those from literature, with those calculated using the temperature dependence, eq 11: \blacktriangle , ref 9; \circ , ref 10; ∇ , ref 12; \blacktriangledown , ref 13; \square , ref 14; \diamond , ref 16; $+$, this work.

not reliable, the values of this isotherm is not included in the fitting:

$$B_1/(\text{cm}^3 \text{ mol}^{-1}) = 12.729 - 0.00312(T/K)$$

$$B_{12}/(\text{cm}^3 \text{ mol}^{-1}) = 17.85 + 0.0123(T/K)$$

$$B_2/(\text{cm}^3 \text{ mol}^{-1}) = -122.92 + 0.5945(T/K) - 0.0006662(T/K)^2$$

$$C_1/(\text{cm}^6 \text{ mol}^{-2}) = 249.00 - 0.476(T/K)$$

$$C_{112}/(\text{cm}^6 \text{ mol}^{-2}) = 347$$

$$C_{122}/(\text{cm}^6 \text{ mol}^{-2}) = 585$$

$$C_2/(\text{cm}^6 \text{ mol}^{-2}) = 2147.9 - 2.54(T/K) \quad (11)$$

4. Summary

In general the uncertainties of the interaction second virial coefficients are somewhat larger than those of the second virial coefficients of the pure components.

In Figures 5–8 we compare eq 11 with the values of virial coefficients of pure helium and pure nitrogen given in Table III, as well as those of the literature quoted by Dymond (6) as class I. Moreover comparison with the results by Duschek (7) has also been made. Generally speaking, our results are close to

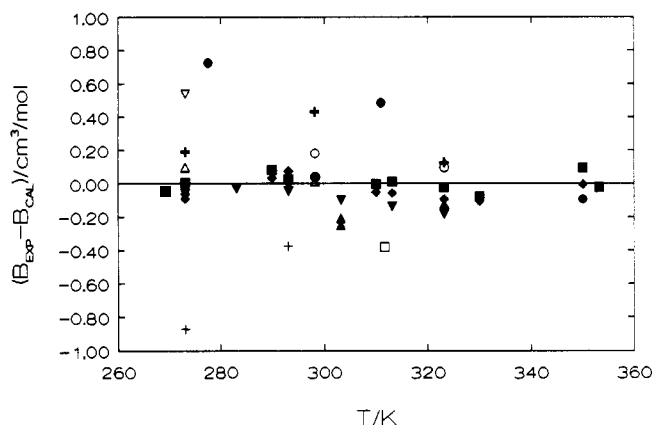


Figure 7. Comparison of the second virial coefficients of pure nitrogen from this work, as well as those from literature, with those calculated using the temperature dependence, eq 11: +, ref 18; Δ , ref 19; \circ , ref 20; +, ref 21; \blacktriangle , ref 10; \bullet , ref 25; ∇ , ref 12; \diamond , ref 22; \square , ref 14; \blacktriangledown , ref 7; \blacklozenge , ref 4; \blacksquare , this work.

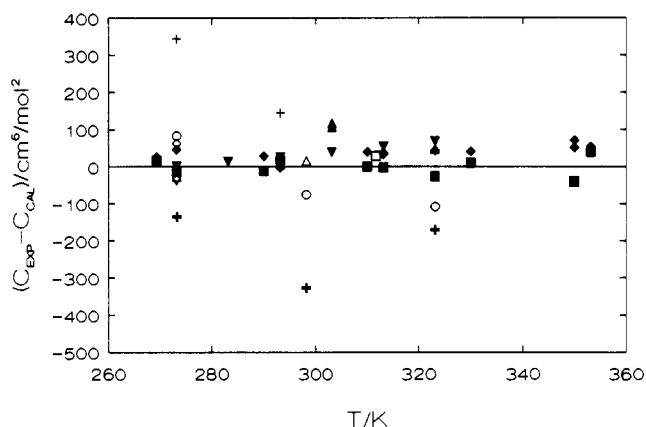


Figure 8. Comparison of the third virial coefficients of pure nitrogen from this work, as well as those from literature, with those calculated using the temperature dependence, eq 11: +, ref 18; Δ , ref 19; \circ , ref 20; +, ref 21; \blacktriangle , ref 10; ∇ , ref 12; \diamond , ref 22; \square , ref 14; \blacktriangledown , ref 7; \blacklozenge , ref 4; \blacksquare , this work.

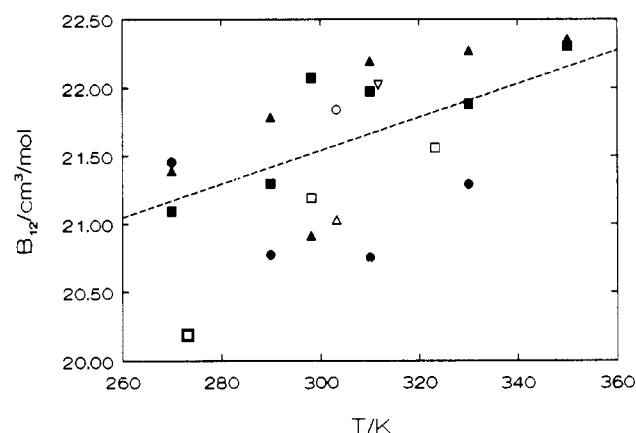


Figure 9. Interaction second virial coefficients of this work and literature: \blacktriangle , this work, 24.94 mol % He; \bullet , this work, 49.96 mol % He; \blacksquare , this work, 74.91 mol % He; Δ , ref 10; \circ , ref 23; ∇ , ref 14; \square , ref 24; --, eq 11.

the average of the previous investigations.

Literature values of B_{12} are limited. The comparison in Figure 9 shows a good agreement of the present work with previous investigations. The results of the mixture with 49.96 mol % helium at 350 K have been omitted from this plot since there is likely some error in the measurement. Unfortunately a comparison for the interaction third virial coefficients is not possible because of a lack of literature data.

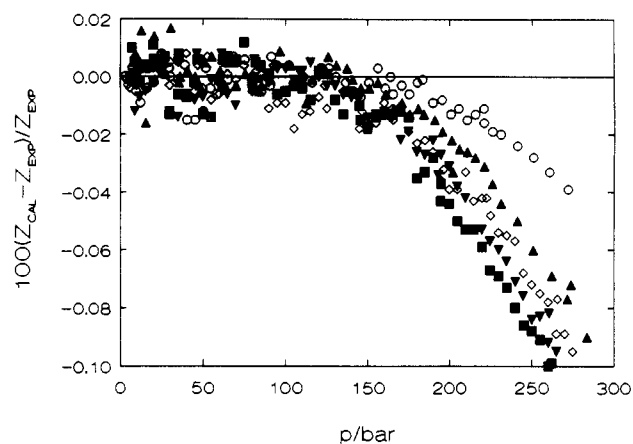


Figure 10. Deviation of the compressibility factor of pure helium calculated with the three-term virial equation of state from the experimental data of this work: \circ , 273.15 K; \blacktriangle , 293.15 K; \diamond , 313.15 K; \blacktriangledown , 330.00 K; \blacksquare , 353.15 K.

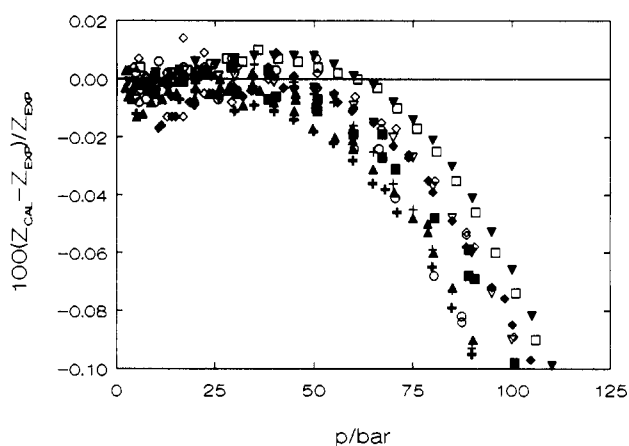


Figure 11. Deviation of the compressibility factor of pure nitrogen calculated with the three-term virial equation of state from the experimental data of Jaeschke et al. (3, 4): +, 269.30 K; \circ , 273.15 K; +, 290.00 K; \blacktriangle , 293.15 K; ∇ , 310.00 K; \diamond , 313.15 K; \square , 323.15 K; \blacktriangledown , 330.00 K; \blacklozenge , 350.00 K; \blacksquare , 353.15 K.

In Figures 10 and 11, we compare the compressibility factor predicted by eq 11 with experimental data. It is shown that this temperature dependence of B and C , eq 11, describes the PVT behavior of pure helium up to 200 bar with a deviation of less than 0.05%, and the same is true for nitrogen, only up to about 80 bar. For the mixtures it is somewhere between 80 and 200 bar, depending on the composition of the mixtures.

Acknowledgment

We thank Prof. C. A. ten Seldam for his assistance with the preliminary data processing. Our thanks go to Dr. S. N. Biswas as well for the stimulating discussion. This is the 435th publication of the Van der Waals Laboratory.

Glossary

a, b	pressure distortion coefficients
$A_n, B_n,$	1st, 2nd, and 3rd refractive virial coefficients
C_n	
$B, C,$	2nd, 3rd, 4th, and 5th virial coefficients, respectively
D, E	
$c_1, c_2,$	coefficients of eq 7
c_3	

<i>L</i>	cell length
<i>n</i>	refractive index number
<i>N</i>	cell constant
<i>P</i>	pressure
<i>T</i>	temperature
<i>V</i>	volume
<i>x</i>	mole fraction
Z_0/P_0	run constant
<i>Z</i>	compressibility factor

Abbreviations

BUR	Burnett experiment
DPM	differential pressure meter
eq	equation
eqs	equations
OPT	optical experiment
PEC	pressure equilibrium chamber

Greek Letters

Δ	uncertainty
λ	wavelength
ρ	density
σ	standard deviation

Subscripts

0	initial condition
1, 2	components of helium and nitrogen, respectively
<i>i, j</i>	gas expansion number
mix.	mixture

Superscript

0	condition of zero pressure
---	----------------------------

Registry No. N₂, 7727-37-9; hydrogen, 1333-74-0.

Literature Cited

- (1) Vos, W. L.; Schouten, J. A. *Phys. Rev. Lett.* **1990**, *64*, 898.
- (2) Jaeschke, M. *Int. J. Thermophys.* **1987**, *8*, 84.
- (3) Jaeschke, M.; Humphreys, A. E. *The GERG Data Bank of High Accuracy Compressibility Factor Measurements*; GERG Technical Monograph TM4; Verlag des Vereins Deutscher Ingenieure, Düsseldorf, 1990. *Fortschr.-Ber. VDIZ., Reihe 6*, **1991**, No. 251.
- (4) Jaeschke, M.; Hinze, H. M. *Fortschr.-Ber. VDIZ., Reihe 6*, to be published.
- (5) Van der Berg, H. R. Thesis, University of Amsterdam, 1979.
- (6) Dymond, J. H.; Smith, E. B. *The Virial Coefficients of Pure Gases and Mixtures*; Clarendon Press: Oxford, U.K., 1980.
- (7) Duschek, W.; Kleinrahn, R.; Wagner, W.; Jaeschke, M. *J. Chem. Thermodyn.* **1988**, *20*, 1069.
- (8) Gibby, C. W.; Tanner, C. C.; Masson, I. *Proc. R. Soc.* **1928**, *A122*, 283.
- (9) Michels, A.; Wouters, H. *Physica* **1941**, *8*, 923.
- (10) Pfefferle, W. C., Jr.; Goff, J. A.; Miller, J. G. *J. Chem. Phys.* **1955**, *23*, 509.
- (11) Stroud, L.; Miller, J. E.; Brandt, L. W. *J. Chem. Eng. Data* **1960**, *5*, 51.
- (12) Canfield, F. B.; Leland, T. W.; Kobayashi, R. *Adv. Cryogen. Eng.* **1963**, *8*, 146.
- (13) Hoover, A. E.; Canfield, F. B.; Kobayashi, R.; Leland, T. W., Jr. *J. Chem. Eng. Data* **1964**, *9*, 568.
- (14) Ku, P. S.; Dodge, B. F. *J. Chem. Eng. Data* **1987**, *12*, 158.
- (15) Dillard, D. D.; Waxman, M.; Robinson, R. L., Jr. *J. Chem. Eng. Data* **1978**, *23*, 269.
- (16) Kell, G. S.; McLaurin, G. E.; Whalley, E. *J. Chem. Phys.* **1978**, *68*, 2199.
- (17) Prasad, M.; Kudchadker, A. P. *J. Chem. Eng. Data* **1978**, *23*, 190.
- (18) Verschoyle, T. T. H. *Proc. R. Soc.* **1926**, *A111*, 552.
- (19) Otto, J.; Michels, A.; Wouters, H. *Z. Phys.* **1934**, *35*, 97.
- (20) Michels, A.; Wouter, H.; De Boer, J. *Physica* **1934**, *1*, 587.
- (21) Michels, A.; Lunbek, R. J.; Wolkers, G. J. *Physica* **1951**, *17*, 801.
- (22) Grain, R. W., Jr.; Sonntag, R. E. *Adv. Cryogen. Eng.* **1966**, *11*, 379.
- (23) Kramer, G. M.; Miller, J. G. *J. Phys. Chem.* **1957**, *61*, 785.
- (24) Brewer, J.; Vaughn, G. W. *J. Chem. Phys.* **1969**, *50*, 2960.
- (25) Gunn, R. D. M.S. Thesis, University of California (Berkeley), 1958.

Received for review May 29, 1991. Accepted August 14, 1991.

Supplementary Material Available: Tables of experimental compressibility factors of the binary system of helium and nitrogen, containing raw data which were obtained in Burnett and optical experiments (10 pages). Ordering information is given on any current masthead page.